Journal of Neurophysiology, Accepted on June 23, 2008

Title: Neuro-Musculo-Skeletal Torque Generation Process Has a Large Destabilizing Effect on the Control Mechanism of Quiet Standing

Abbreviated Title: Neuro-Musculo-Skeletal System in Controlling Quiet Standing

Authors: Kei Masani[1,2], Albert H. Vette[1,2], Noritaka Kawashima[1,2,3], Milos R. Popovic[1,2]

[1] Rehabilitation Engineering Laboratory,
Institute of Biomaterials and Biomedical Engineering, University of Toronto
164 College Street, Toronto, ON, M5S 3G9, Canada

[2] Rehabilitation Engineering Laboratory,
Lyndhurst Centre, Toronto Rehabilitation Institute
520 Sutherland Drive, Toronto, ON, M4G 3V9, Canada

[3] Japan Society for the Promotion of Science,
6 Ichibancho, Chiyoda-ku, Tokyo 102-8471, Japan;

Corresponding Author:
Kei Masani PhD
Rehabilitation Engineering Laboratory, Lyndhurst Centre,
Toronto Rehabilitation Institute
520 Sutherland Drive, Toronto, ON, M4G 3V9, Canada
Phone: +1-416-597-3422 ext 6098 / Fax: +1-416-425-9923
E-mail: k.masani@utoronto.ca

Number of figures and tables: 8 Figures, 1 Table
Number of pages: 36 pages including Figures and Table

Abstract

The delay of the sensory-motor feedback loop is a destabilizing factor within the neural control mechanism of quiet standing. The purposes of this study were 1) to experimentally identify the neuro-musculo-skeletal torque generation process during standing posture, and 2) to investigate the effect of the delay induced by this system on the control mechanism of balance during quiet standing. Ten healthy adults participated in this study. The ankle torque, ankle angle, and electromyograms from the right lower leg muscles were measured. A ground-fixed support device was used to support the subject at his/her knees, without changing the natural ankle angle during quiet standing. Each subject was asked to mimic the ankle torque fluctuation by exerting voluntary ankle extension while keeping the supported standing posture. Utilizing the rectified soleus electromyogram as the input and the ankle torque as the output, a critically damped, second-order system (twitch contraction time of 0.152±0.027 s) successfully described the dynamics of the torque generation process. According to the performed Bode analysis, the phase delay induced by this torque generation process in the frequency region of spontaneous body sway during quiet standing was considerably large, corresponding to an effective time delay of about 200 to 380 ms. We compared the stability of the balance control system with and without the torque generation process, and demonstrated that a much smaller number of gain combinations can stabilize the model with the torque generation process than without it. We concluded that the phase delay induced by the torque generation process is a more destabilizing factor in the control mechanism of quiet standing than previously assumed, which restricts the control strategies that can stabilize the entire system.

Introduction

In the research field of human bipedal stance, many studies have focused on the control mechanism of the ankle joint torque during quiet standing, since the ankle joint has the primary role of maintaining center of mass (COM) equilibrium during standing. Due to the fact that the COM is in front of the ankle joint during the natural standing posture, a gravity-induced torque continuously accelerates the body forward from the upright position. Therefore, a corrective ankle extension torque is continuously required to resist the gravity effect and to ensure that the COM remains close to the equilibrium position.

The discussion on this process of corrective torque regulation is controversial. The corrective torque can be evoked actively and passively. Passive torque components are the result of intrinsic mechanical properties, i.e., stiffness and/or viscosity, produced by muscle and surrounding tissue, whereas active torque components are the result of the muscle activity regulation via the neural employment of sensory and motor systems. It has been reported that passive torque components alone are not sufficient to provide the required corrective torque (Morasso and Sanguineti, 2002; Loram and Lakie, 2002; Casadio et al., 2005). Additionally, numerous studies have demonstrated that quiet stance posture can be perturbed by stimulating various sensory systems (e.g., Fitzpatrick et al. 1992a,b, 1994, 1996; Fitzpatrick and McCloskey, 1994; for review, Horak and Macpherson 1996). These findings imply that, in addition to the passive torque components, the active control mechanism must necessarily contribute to the corrective torque generation.

The nature of the active control mechanism during quiet standing is not fully understood either. One of the key questions is whether a feedback mechanism (Masani et al., 2003, 2006a; Peterka, 2002; Peterka and Loughlin, 2004; Cenciarini and Peterka, 2006; Mergner et al. 2003) or a feedback with a predictive mechanism (Fitzpatrick et al., 1996; Morasso et al. 1999; van der Kooij et al. 1999, 2001) plays the primary role. Regardless of the control mechanism, the delay in the control system is one of the major destabilizing factors. For

example, Morasso and Schieppati (1999) suggested that a time delay of about only 50 ms is sufficient to threaten the stability of a human size inverted pendulum, if a simple linear control mechanism is used to regulate balance. Therefore, the performance of the control mechanism must be carefully evaluated given the delay in the loop. In most analytical studies that use models to simulate bipedal stance, the delay in the feedback loop has been considered as being constant. Various values for the time delay have been suggested, but most of them are in the range from 80 to 100 ms (Jo and Massaquoi 2004; Masani et al., 2006a; van der Kooij et al., 1999, 2001; Peterka, 2000). These values are supposed to represent the delays due to the neural transmission and the neuro-musculo-skeletal (NMS) torque generation process. However, the transcortical round trip signal transmission delay already consumes about 80 ms. As such, researchers seem to have considered solely the neural transmission delay while ignoring the delay due to the NMS torque generation process.

To date, no study has investigated the effect of the delay induced by the NMS torque generation process on the control mechanism of balance during quiet standing. The model of the NMS torque generation process for an isometric torque exertion task could also be used for the standing task, since the muscle length change is very small during quiet standing, i.e., only 0.4 % of the full potential length change (0.6 mm in Loram et al., 2005, compared to 140 mm in Kawakami et al., 1998). For the isometric task, the NMS torque generation process has been concisely modeled as a critically damped, second-order system (Stein et al., 1972; Fuglevand and Winter 1993). Note that the second-order dynamics induce a *phase delay* as a function of frequency instead of a constant *time delay*. The phase delay of the second-order system is monotonically increasing, i.e., the higher the frequency, the larger the phase delay. Considering that spontaneous body sway during quiet standing is one of the slowest body movements far below 1 Hz, and that the corresponding motor command must include similarly slow components, the phase delay induced by the NMS torque generation process must be small as well. However, we should consider that, since

the lower frequency components have a longer period, the small phase delay of the low frequency components might have a large absolute time delay effect (*effective time delay*). For example, when a phase delay at 5 Hz is 150 deg, the effective time delay of this frequency component is 0.083 s. However, when a phase delay at 0.5 Hz is 50 deg, the effective time delay of this component is 0.278 s. As such, the effective time delay induced by a slow body sway movement during quiet standing can be potentially large.

In the case that the NMS system is modeled as a critically damped, second-order system, the system dynamics are uniquely characterized by its *natural frequency*. The natural frequency is equivalent to the inverse of the muscle *twitch contraction time* (Fuglevand and Winter, 1993; Winter 2005), which represents the time interval from the moment when a stimulus arrives at the muscle to the moment when the generated force reaches its peak. Tani and Nagasaki (1996) used a voluntary impulsive plantar flexion task during sitting to measure the twitch contraction time in the soleus muscle, reporting a value of 86 ms. Bellemare et al. (1983) identified a value of 116±9 ms using supramaximum electrical stimulation during sitting, whereas Buchthal and Schmalbruch (1970) reported a value of 74 (52-100) ms using submaximum electrical stimulation during sitting. Thus, the reported values in the literature were obtained during sitting when the joint condition is very different from that during standing. Additionally, the motor task in these previous studies was also different compared to standing: The impulsive voluntary torque exertion at a level of 30 % maximum voluntary contraction (Tani and Nagasaki, 1996) and the electrical stimulation (Bellemare et al.,1983; Buchthal and Schmalbruch, 1970) must include a higher level of fast fiber activity than the ankle torque exertion during quiet standing. Since the delay induced by the NMS system is due to the chemical and mechanical muscle and joint dynamics, the twitch contraction time is believed to depend on the muscle fiber properties involved in the corresponding motor task, and on the ankle joint and foot condition, such as the joint angle, the pressure on ligaments, and the foot stiffness. Therefore, it was required to identify the NMS system under a condition equivalent to the quiet standing posture.

The purposes of this study were 1) to experimentally identify the NMS system during standing posture, and 2) to theoretically investigate the delay effect of this component on the control mechanism of balance during quiet standing. A part of this study was published as an abstract (Masani et al. 2006b).

Methods

Experimental Study

Subjects

Ten healthy adults (9 male and 1 female; age 21-39 years; height 174±7.0 cm; weight 71.7±11.2 kg) participated in this study. They had no medical history or signs of neurological disorders. All subjects gave their written informed consent to participate in the study after receiving a detailed explanation about the purposes, benefits, and risks associated with the participation in the study. The experimental procedures used in this study were approved by the local ethics committee.

Measurements

The center of pressure (COP) and three orthogonal components of the ground reaction force were measured using a force platform (Accu Sway ACS-DUAL, Advanced Mechanical Technology Inc., USA). The force platform was a split force platform, which measured the forces exerted by each foot separately. Surface electromyograms (EMG) were recorded from the right soleus muscle (SOL), medial (MG) and lateral (LG) heads of the gastrocnemius muscle, and the tibialis anterior muscle (TA). The EMGs were amplified and bandpass filtered between 20 and 500 Hz (Bangnoli 8 EMG System, Delsys, U.S.A.). The displacement of a point on the shank (Fig. 1) was measured by a charge coupled laser displacement sensor (LK-2500, Keyence, Japan). All data were sampled at 1 kHz and stored on a personal computer for subsequent analysis. In this paper, we focus only on the anteroposterior body sway, since the ankle extensors contribute primarily to the

stabilization of the body sway in this direction.

The ankle angle was calculated using the laser displacement sensor data, under the assumption that the feet did not move on the force plate during standing. The exerted torque at the ankle joint was calculated using COP and the ground reaction forces.

Tasks

To identify the NMS system during quiet standing, we adopted a unique experimental setup. As shown in Fig. 1, the ground-fixed support device was used to externally counteract the toppling effect of gravity during standing, eliminating the requirement of the joint torque exertion. Using this procedure, a standing posture without the presence of muscle activity and without ankle joint movement was realized.

The first task, which we refer to as 'free standing (FS)', was the actual quiet standing task. The second task represented standing when utilizing the support device. We refer to this task as 'supported standing (SS)'. This task was used to test whether 1) the muscle activity was close to the resting level, and 2) the support device provided most of the average quiet standing torque when using the device. A load cell was built in to measure the load exerted on the support device. During SS, an experimenter positioned the support device just below the subject's patellas of both legs. Note that the support device was positioned without changing the natural ankle angle of quiet standing. Since most of the required ankle torque against the gravity toppling torque was exerted by the support device under the SS condition, the activity of the ankle extensors was attenuated and the calculated ankle torque became close to zero (see Results). Thus, we actualized that the subject stood with the same average ankle angle as that of FS without activating the ankle muscles. During the third task, the subject assumed the same position as in SS, but voluntarily exerted ankle extension torque in a random manner to mimic the torque fluctuation during FS. We refer to this task as 'voluntary task standing (VS)'. Prior to this task, the subject watched the recording of the force fluctuation during FS and practiced this task. The subject was instructed to exert an ankle force that mimicked the force fluctuation during FS by

focusing on its randomness and amplitude. The subject was also instructed not to reduce the load on the support device to zero, which could result in a detachment of his/her shank from the supporting device and in a change of the ankle angle. Thus, we obtained the relationship between the activity of the ankle extensors and the corresponding active ankle torque during standing posture.

In all tasks, the subject stood with bare feet and eyes closed, the arms hanging along the sides of the body, and the heels 15 cm apart. The subject did not change the position of the feet between the trials while he/she sat down on a chair in order to take a rest. One trial for each task was executed. The duration of each trial was 120 s for FS and VS, whereas the duration of SS was 30 s. The resting EMG was recorded in a sitting posture for 30 s. The recording length of 120 s for FS and VS was selected to reliably capture the fluctuation characteristics of body sway (Carpenter et al. 2001), whereas the recording length of 30 s for SS and the resting EMG was assumed to be sufficient for the calculation of the average muscle activity level.

Data Analysis

Before identifying the NMS system, we tested 1) if the average ankle angle was kept the same among the three standing conditions; 2) if the average ankle torque in VS and the average torque provided by the support device in SS were the same as the average ankle torque in FS; 3) if the activity of each muscle was sufficiently attenuated by the use of the support device during SS; and 4) if the activity of each muscle in VS was consistent with that in FS. The ankle torque, the torque provided by the support device and the ankle angle were assessed by calculating the mean values. The muscle activity was assessed by calculating the root mean square of the EMGs. Statistical comparisons among tasks were performed by an ANOVA with repeated-measures and a Tukey-Kramer multiple comparisons test (Statview ver. 5.0, SAS Institute Inc., USA). $P < 0.05$ was used as the level of statistical significance.

The ankle extensors are responsible for generating the active ankle torque, since the

ankle extensors show continuous activity whereas the ankle flexors are silent or only intermittently active. Among the ankle extensors, it has been reported that SOL activity during quiet standing is about 5 % and gastrocnemius activity about 1 % of their maximum activity (Panzer et al., 1995). Indeed, in our experiments, SOL activity was continuously observed, but MG and LG activity was phasic and small, or rarely observed. Additionally, the cross-sectional area of SOL is twice as large as the total area of MG and LG (Yamaguchi et al., 1990). Therefore, we assumed that, in standing, the SOL contribution to the generation of the ankle torque is much larger than the MG and LG contribution, even when the differences in fiber type among the muscles are considered (Yamaguchi et al., 1990). Thus, we decided to use only rectified SOL EMG for the identification of the NMS system in this study. It was required, however, that the random muscle activity and resulting ankle torque fluctuation during VS (corresponding to the input and output of the NMS system, respectively) mimic the fluctuations during FS. In order to confirm this, we compared the frequency spectrum of the rectified SOL EMG as well as of the ankle torque between FS and VS.

We modeled the transfer function from rectified EMG to ankle torque using a critically damped, second-order system (Stein et al., 1972; Fuglevand and Winter, 1993). From a physiological perspective, the second-order dynamics represent the chemical dynamics due to the variation of calcium concentration in the muscle fiber and the mechanical dynamics due to the sliding filament action (Bobet et al., 1998; Zajac, 1989). The transfer function ($H(s)$) is written as:

$$H(s) = \frac{G\omega_n^2}{(s+\omega_n)} = \frac{G(1/T)^2}{(s+1/T)^2}, \tag{1}$$

where G is the gain, ω_n the natural frequency of the second-order system, and T the twitch contraction time. The dynamic characteristics of eq. (1) are determined by the natural frequency, which corresponds to the inverse of the twitch contraction time of the muscle

(T=1/ω_n). G on the other hand depends on the location of the electrodes and the impedance between the electrodes and the skin. Therefore, G has no deeper physiological meaning in the context of the present study and will not be discussed any further. Note that ω_n and T equivalently capture the characteristics of the NMS system. Since the twitch contraction time is more familiar in the physiology field, we only used the twitch contraction time hereafter.

The variables of the transfer function, T and G in eq. (1), were optimized by means of the DIRECT optimization technique to yield matching between the estimated and experimental ankle torque in VS (Matlab ver. 7.0.4R14SP2, Mathworks Inc., USA; and Simulink ver. 6.2R14SP2, Mathworks Inc., USA). Note that the DIRECT optimization technique is a sampling algorithm that requires no knowledge of the objective function gradient. Instead, the algorithm samples points in the domain and uses the information it has obtained to decide where to search next. The search range for T was set to $0.040 < T < 0.200$ s, with an initial value of $T = 0.100$ s. We used the latter 60 s of the VS data for the optimization (optimized data), and the first 60 s of the VS data for the validation of the optimized function (validation data). Our objective of the analysis was to assess the goodness of fit between the measured ankle torque (y_i) and the torque estimated from rectified SOL EMG using the transfer function (Y_i). The goodness of fit was determined by calculating the average of the percentage errors for all samples using:

$$\%Fit = 100 \times (1 - \frac{1}{N}\sum_{i=1}^{N}\left|\frac{y_i - Y_i}{y_i}\right|) \qquad (2)$$

where N is the number of points.

Theoretical Study

We theoretically investigated the delay effect of the experimentally identified NMS system on the control mechanism of balance during quiet standing. At first, the amplitude and

phase responses of the identified transfer functions were determined using Bode analysis. G in eq. (1) was set to 1 to isolate the frequency-specific properties of the transfer function in this Bode analysis. To examine the effect of the inter-subject variability on the NMS system, we tested three transfer functions with 1) group average T, 2) group maximum T, and 3) group minimum T.

Next, we implemented the identified NMS system into a model that included a model of human bipedal stance and a model of its potential control mechanism, and tested the stability of the system. In the current study, we adopted a feedback control mechanism with linear controllers, which was based on work by Peterka (2002). Note that the stability of this system is more affected by the feedback delays compared to the control mechanism with a predictive mechanism. The model was based on the following assumptions: 1) Quiet standing posture was approximated as a single link inverted pendulum; and 2) the ankle torque was controlled by a mechanical and a neural controller, both of which were linear controllers (PD, i.e., proportional and derivative controllers). The mechanical controller provided the passive torque components, whereas the neural controller provided the active torque components.

We tested the stability of the entire system consisting of the controllers, an inverted pendulum representing human bipedal stance, transmission time delays, and the NMS system. Fig. 2 shows the block diagram of the system used in this stability test. The size of the inverted pendulum was equivalent to the group average of the subjects in this study, i.e., m = 69.8 kg, I = 59.5 kgm^2, h = 0.902 m. Eight out of 10 subjects (see Results of the experimental study) were used for the calculation of m, I, and h, which was based on Winter (2005). m was defined as $m = 0.971M$ where M indicates the subject's body mass. h was defined as h=$0.261l_1$+$0.945l_2$ where l_1 indicates the trunk length and l_2 indicates the leg length. I was defined as $I = 0.678M(0.374l_1 + l_2)^2 + 0.192Ml_2^2$. The neural controller consisted of a proportional gain, K_P, and a derivative gain, K_D. The mechanical controller

provided the rotational stiffness K and the rotational viscosity B.

While the output of the mechanical controller directly translated into the passive ankle torque, the output of the neural controller was delayed by a constant time delay (τ) and the NMS system generating the active ankle torque. The sensory feedback time delay that represents the cumulative time loss due to neural transmission from the ankle somatosensory system to the brain was suggested to be 35 to 40 ms, determined by a sensory evoked potential method (Applegate et al., 1988). Thus, we selected 40 ms for the sensory feedback time delay. The motor time delay represented the cumulative time loss due to the CNS decision making process and the neural transmission from the brain to the ankle extensors. Although the motor time delay from the cortex to the soleus was suggested to be about 27 to 37 ms determined by a motor evoked potential method (Ackermann et al., 1991; Lavoie et al., 1995), there is no information regarding the CNS decision making process in the literature. Thus, we used the same value as for the sensory feedback time delay (40 ms), which represents the minimum physiological value. Thus, a total constant time delay (τ) of 80 ms was implemented. Note that this value was approximately the same as in previous studies (Jo and Massaquoi, 2004; Masani et al., 2006a; van der Kooij et al., 1999, 2001; Peterka, 2000).

For each of the three tested T values (see above), we systematically changed K_P, K_D, and K in the ranges of $0 \leq K_P \leq 2000$ Nm/rad, $0 \leq K_D \leq 2000$ Nms/rad, and $0 \leq K \leq 2000$ Nm/rad with a step size of 20 for each. Based on Loram et al. (2002), B was set to $B = 0$, 5 and 10 Nms/rad. However, since these small differences in B did not show a large effect on the results, only the results obtained for $B = 5$ are presented in this paper.

We performed Nyquist stability analysis with the open-loop system (framed in by the thick dashed box in Fig. 2) in order to test the stability of the closed-loop system. For comparison purposes, the same analysis was performed for the control system without the NMS system.

Results

Experimental Study

Fig. 3 shows the recorded time series for a single subject. Note that, for FS and VS, only the first 60 s of the analyzed 120 s are presented in the figures in order to isolate the signal features. The top row compares the ankle angle among the tasks. The average ankle angles during SS and VS were about the same as during FS, and their fluctuations were almost constant compared to that of FS. The small fluctuation of the ankle angle in VS was due to the effect of soft tissue around the knee joints of the subject. The second row in Fig. 3 compares the ankle torque among the tasks. The ankle torque during SS (bold line) was much smaller than that of FS, and was close to zero. On the other hand, the torque provided by the support device (thin line with $*$) was about the same as that of FS. In VS, the ankle torque was similar but slightly smaller than that of FS. The torque provided by the support device was not decreased to zero, which indicates that the shank was never detached from the supporting device. The bottom four rows in Fig. 3 compare the muscle activities among the tasks and the resting condition. The muscle activity of the ankle extensors, especially of SOL and MG, was attenuated during SS and about identical to the resting condition. In VS, the SOL and MG EMGs seemed as large as those in FS. The activity of LG and TA was as small as during the resting condition, except for bursts occurring a few times during the entire recording. As two out of 10 subjects did not show the obvious attenuation of the SOL activity during SS, the subsequent analysis was performed without these subjects.

The group averages (mean±SD) of the measured ankle angles were 0.0787±0.0166, 0.0820±0.0326, and 0.0841±0.0331 rad for FS, SS, and VS, respectively. There was no statistically significant difference in ankle angle among the tasks (P = 0.730). Fig. 4 A shows the average torque in FS, VS and SS. There was no statistically significant difference in the torque among the tasks (P = 0.568). Fig. 4 B, C, D, and E show the rectified EMGs in FS, SS, VS and the resting condition. Except for TA, there were significant differences

among the conditions ($P < 0.0001$, = 0.001, 0.0017, 0.111 for SOL, MG, LG, TA, respectively). For SOL, MG, and LG, there was no significant difference between FS and VS, and between SS and the resting condition.

Fig. 5 shows the power spectral density functions of the rectified SOL EMG (A) and the ankle torque (B) for all subjects during FS and VS. The frequency range of both time series and the amount of the power was approximately identical for the FS and VS tasks. This indicates that each subject's voluntary torque exertion successfully mimicked that of spontaneous body sway.

The measured ankle torque and the ankle torque estimated from rectified SOL EMG (VS) using the identified NMS system were compared in Fig. 6 for one subject. Note that the estimated ankle torque (bold lines in the torque plots) fitted the measured ankle torque (thin lines in the torque plots) very well, both in the optimized (A) and the validation data (B). Table 1 summarizes the results of the optimization analysis. The %Fit was quite high in both of the optimized and the validation data (89.9 and 87.6 %, respectively), and no difference in %Fit between the optimized and the validation data was found (paired *t*-test, $P = 0.094$). The average twitch contraction time was $T = 0.152 \pm 0.027$ s, and the group minimum and maximum values were $T = 0.121$ and $T = 0.192$ s, respectively.

Theoretical Study

Fig. 7A and B show the Bode plots of the identified NMS systems. The cut-off frequencies at 3 dB were below 1 Hz: 0.845, 0.673, 0.532 Hz for T=0.121,0.152, and 0.192 s, respectively. In other words, the gains below 1 Hz were close to the second-order function's gain G (Fig. 7A). However, the phase delay in this frequency region was considerable (Fig. 7B). At the cut-off frequency, the phase delays were -66.0, -69.9, and -72.7 deg for T = 0.121,0.152, and 0.192 s, respectively. Fig. 7C shows the effective time delays for each frequency component based on the phase delay. The effective time delay below 1 Hz was between 0.200 s and 0.380 s. At the cut-off frequency, the effective time delays were 0.215,

0.265, and 0.331 s for T = 0.121,0.152, and 0.192 s, respectively. For the purpose of comparison, Fig. 7D and E show the empirical frequency response function for the same subject as in Fig. 6. The shape of the gain and phase functions is similar to the Bode plots (Fig. 7A and B), i.e., the cut-off frequency at 3 dB was 0.549 Hz, the phase delay at the cut-off frequency was -35.9 deg, and the effective time delays for the frequency components below the cut-off frequency ranged from 0.640 to 0.181 s.

Fig. 8A shows the three-dimensional volume plot of the gain combinations of K_P, K_D and K that stabilized the entire model including the NMS system with T = 0.152 s. Fig. 8B, C and D represent the projections of those gain combinations onto the planes of K_P and K_D (Fig. 8B), K_P and K (Fig. 8C), and K_D and K (Fig. 8D) that stabilized the entire model including the NMS system with T = 0.121 s (red +), T = 0.152 s (yellow ×), and T = 0.192 s (blue). The plots indicate, for example, that the neural gain combination of K_P=300 and K_D=460 can stabilize the whole system only for T = 0.121, but not for T = 0.152 s or T = 0.192 s. Fig. 8E, F, and G show the projections of those gain combinations onto the planes of K_P and K_D (Fig. 8E), K_P and K (Fig. 8F), and K_D and K (Fig. 8G) that stabilized the entire model without the NMS system (grey area enclosed by dotted lines) compared to the stabilizing gain combinations with the NMS system (red +: T = 0.121 s, yellow ×: T = 0.152 s, and blue : T = 0.192 s).

When the model with the NMS system is compared with the model without the NMS system (Fig. 8E, F, and G), the grey areas enclosed by the dotted lines (without the NMS system) are much larger than the areas covered by the other symbols (with the NMS system). For example, the neural gain combination of K_P=1000 and K_D=400 can stabilize the model without the NMS system, whereas the same neural gain combination cannot stabilize the model with the NMS system - no matter how larger the mechanical stiffness is. This result indicates that a much smaller number of gain combinations can stabilize the

model with the NMS system compared to the model without it. For the model with the NMS system, a smaller area is covered for a larger T in all Fig. 8B, C, and D. This result indicates that a lower number of stabilizing gain combinations was identified for the model with the NMS system when T got larger.

Discussion

It was demonstrated that the activity of the ankle extensors in SS was attenuated to the level of the resting condition with keeping the same average ankle angle as during FS, since the gravity toppling torque was successfully compensated for by the support device (Fig. 4). Hence, it was realized that the subject stood in a natural standing posture without exerting any muscle induced ankle torque. Taking advantage of this condition, we obtained the relationship between SOL EMG and the ankle torque in VS, which both had the same magnitude (Fig. 4) and spectral features (Fig. 5) as those in FS. Subsequently, the NMS system was successfully identified as a critically damped second-order system (Fig. 6 and Table 1). When we focused on the frequency region of body sway in the Bode plots of the identified NMS system (below 1 Hz), we found that the motor command, which has similar frequency characteristics as body sway, is transferred through the NMS system without being damped (Fig. 7A). On the other hand, the phase delay was considerable in this frequency region (Fig. 7B). When the phase delay was translated into the effective time delay for each frequency component to investigate the delay effect, the corresponding time delay was between 200 and 380 ms for the frequency region of body sway (Fig. 7C). This suggests that the NMS system causes a large delay in the control mechanism. As a result, the stability analysis revealed that a much smaller number of gain combinations can stabilize the model with the NMS system compared to the model without the NMS system (Fig. 8). Additionally, a lower number of gain combinations was able to stabilize the entire model with the NMS system when T was larger.

Identification of the NMS System

To investigate the delay effect of the NMS system on the control mechanism of quiet standing, it was required to identify the NMS system for a condition that is equivalent to standing posture. Since the reported twitch contraction time values in the literature were not applicable (Tani and Nagasaki, 1996; Bellemare et al., 1983; Buchthal and Schmalbruch, 1970), it was decided to identify it particularly for the quiet standing posture. In this study, we identified the NMS system under approximately the same condition as that of standing, taking advantage of the SS condition. Therefore, the NMS system identified in this study is more reliable and appropriate for the investigation of the control mechanism of quiet standing. Note that it is not appropriate to use the relationship between EMG and ankle torque during FS for the identification of the NMS system, since the ankle torque exerted during quiet standing includes the passive torque components as the ankle angle fluctuates. On the contrary, the passive torque components in VS and SS are supposed to be close to zero.

The optimization analysis revealed that a second order critically damped system can model the NMS system during quiet standing very well (Table 1). The identified twitch contraction time of SOL ranged from 121 to 192 ms, which was longer than the reported values (74 to 116 ms) in the literature (Tani and Nagasaki, 1996; Bellemare et al., 1983; Buchthal and Schmalbruch, 1970). Tani and Nagasaki (1996) also compared the twitch contraction time among 10 to 60 % of maximum voluntary contraction tasks, and reported that a smaller torque exertion tends to relate to a longer twitch contraction time. Since the twitch contraction time depends on the joint condition and the involved muscle fiber types, the differences between the values can be explained by the difference in posture and motor task. In particular, the longer twitch contraction time during quiet standing is most likely due to the small torque exertion during quiet standing, primarily involving slow muscle fibers.

Delay in the Control Mechanism

In the literature, the delay in the active control mechanism has been mostly considered as a constant time delay of about 80 to 100 ms (Jo and Massaquoi, 2004; Masani et al., 2006a; van der Kooij et al., 1999, 2001; Peterka 2000). The neural transmission delay of 80 ms, which consumes a large part of this value, depends on the neural conduction velocity and the body dimensions. Indeed, the neural transmission delay was experimentally estimated to be about 80 ms. The motor delay from the cortex to the soleus was suggested to be about 27 to 37 ms, determined by a motor evoked potential method (Ackermann et al., 1991; Lavoie et al., 1995). The sensory delay from the foot to the cortex was suggested to be 35 to 40 ms, determined by a sensory evoked potential method (Applegate et al., 1988).

We demonstrated that the NMS system induces an additional large delay, which corresponds to 200 to 380 ms in the case of quiet standing control. Note that this delay is much larger than the neural transmission delay. As such, we revealed that the NMS system is a large delay source for quiet standing control, although it has been almost ignored in previous studies.

Peterka (2002) experimentally identified a constant time delay in the control mechanism of quiet standing. The identified constant time delay, which must include the effect of the NMS system, was about 100 to 200 ms as identified using a mechanical perturbation with frequency components below 2.23 Hz. However, according to our estimation, the total time delay corresponds to about 280 to 460 ms below 1 Hz, which appears longer than his estimation. Since the phase delay is a function of frequency, the frequency of the muscle activity fluctuation affects the identification. Therefore, considering a frequency depending delay in the model would improve the feedback delay identification.

In our previous study (Masani et al., 2006), we demonstrated that a PD controller can robustly stabilize the body even with a time delay up to 185 ms, which is shorter than the time delay effect of the NMS system. However, since we investigated the potential of a PD controller in the previous study, we did not include the passive control mechanism in the

model. Therefore, the control system could only compensate for a delay of up to 185 ms.

Only one study (Jo and Massaquoi, 2004) to date included a critically damped, second-order system in the model. In their study, the linear feedback controllers can stabilize the body against a mechanical perturbation, even though the mechanical controller was very small, i.e., only 90 Nm/rad. However, although they included a critically damped second-order system as the NMS system, a natural frequency of 30 rad/s corresponding to a twitch contraction time of only 33 ms was used for the NMS system. These values represent a much larger natural frequency and a shorter twitch contraction time compared to the results in this study. Thus, the delay effect induced by the NMS system in their study must be very small, and therefore did not cause a problem in the control mechanism of balance during the transient response to a perturbation.

Effect of the NMS System on the Control Mechanism of Balance

The result of the theoretical study supports the conclusion that the phase delay induced by the NMS system is a large destabilizing factor in the control mechanism of quiet standing. Since the phase delay threatens the stability of the system, many gain combinations failed to stabilize the upright posture model when the NMS system was included. Additionally, with a longer twitch contraction time, the number of successful gain combinations was even further limited.

In the field of balance control, it has been argued over the fact whether the active control mechanism of quiet standing acts as a feedback mechanism or rather a feedback with a predictive mechanism (Masani et al., 2003, 2006a; Peterka, 2002; Peterka and Loughlin, 2004; Cenciarini and Peterka, 2006; Mergner et al. 2003; Fitzpatrick et al., 1996; Morasso et al. 1999; van der Kooij et al. 1999, 2001). Although this study does not focus on this question, we emphasize here that the argument should be heavily influenced by the significant phase delay of the NMS system as it represents a destabilizing factor regardless of the control mechanism. In this study, we tested only the feedback mechanism without a predictive mechanism in the controllers. We found that, even without a predictive

mechanism, the feedback mechanism can overcome the delays and stabilize the body. However, it should be noted that we are not implying in this study that feedback control plays the primary role in the actual physiological control system of quiet standing. Instead, we demonstrated that the feedback mechanism has the capacity to regulate balance on its own, i.e., without the contribution of a feed-forward component. Nevertheless, the predictive or feed-forward mechanism is definitely a potential candidate as well. Further investigation is required to determine the extent to which the physiological control mechanism of quiet standing is driven by feedback and feed-forward components. In any case, when such a study is conducted, one needs to take the effects of the NMS system into consideration.

Limitations

We adopted a single muscle model to perform the optimization analysis by assuming that SOL is the most important contributor to the ankle extension torque. The high %Fit in the optimization analysis proved that this assumption was appropriate. However, it has to be noted that MG showed some minor activity as well, which must somehow contribute to the torque generation. Additionally, we used a concise model for the NMS system, i.e., a critically damped second-order system without a constant time delay (Stein et al., 1972; Fuglevand and Winter, 1993). Other more complex models have been proposed, such as a second-order system with a constant time delay (Mannard and Stein, 1973; Ito et al., 2004). Although our optimization results were very good, those more complex models for the NMS system might provide even better results. Hence, the model of the NMS system could be refined in future studies, though the influence of the NMS system on the control mechanism of quiet standing is believed to remain very significant.

Conclusions

We identified the neuro-musculo-skeletal torque generation process in standing posture, taking advantage of the supported standing condition. A critically damped second-order

system (twitch contraction time of 0.152±0.027 s) was successfully used to describe the dynamics of the torque generation process. According to the performed Bode analysis, the phase delay induced by this torque generation process in the frequency region of spontaneous body sway during quiet standing was considerably large, corresponding to an effective time delay of about 200 to 380 ms. By testing the stability of the balance control system, we demonstrated that a much smaller number of gain combinations can stabilize the upright posture model including the torque generation process compared to the model without this component. Thus, we concluded that the phase delay induced by the torque generation process is a large destabilizing factor in the control mechanism of quiet standing, which restricts the control strategies that can stabilize the entire system.

Acknowledgements

We thank Dr. Takayuki Ito and Dr. Alan Morris for their technical assistance. We also thank Professor Jim Taylor and Mr. John Tan for their valuable expertise regarding the stability analysis of linear control system. This work was supported by a grant from the Ministry of Education, Culture, Sports, Science and Technology #12780010 of Japan, the Natural Sciences and Engineering Research Council of Canada, and the Foundation for Total Health Promotion.

References

Ackermann H, Scholz E, Koehler W, and Dichgans J. Influence of posture and voluntary background contraction upon compound muscle action potentials from anterior tibial and soleus muscle following transcranial magnetic stimulation. Electroencephalogr Clin Neurophysiol 81: 71-80, 1991.

Applegate C, Gandevia SC, and Burke D. Changes in muscle and cutaneous cerebral potentials during standing. Exp Brain Res 71: 183-188, 1988.

Bellemare F, Woods JJ, Johansson R, and Bigland-Ritchie B. Motor-unit discharge rates in maximal voluntary contractions of three human muscles. J Neurophysiol 50: 1380-1392, 1983.

Bobet J, and Stein RB. A simple model of force generation by skeletal muscle during dynamic isometric contractions. IEEE Trans Biomed Eng 45: 1010-1016, 1998.

Buchthal F, and Schmalbruch H. Contraction times and fibre types in intact human muscle. Acta Physiol Scand 79: 435-452, 1970.

Carpenter MG, Frank FS, Winter DA, Peysar GW. Sampling duration effects on centre of pressure summary measures. Gait Posture 13: 35-40, 2001.

Casadio M, Morasso PG, and Sanguineti V. Direct measurement of ankle stiffness during quiet standing: implications for control modelling and clinical application. Gait Posture 21: 410-424, 2005.

Cenciarini M, and Peterka RJ. Stimulus-dependent changes in the vestibular contribution to human postural control. J Neurophysiol 95: 2733-2750, 2006.

Fitzpatrick R, Burke D, and Gandevia SC. Loop gain of reflexes controlling human standing measured with the use of postural and vestibular disturbances. J Neurophysiol 76: 3994-4008, 1996.

Fitzpatrick R, and McCloskey DI. Proprioceptive, visual and vestibular thresholds for the perception of sway during standing in humans. J Physiol 478: 173-186., 1994.

Fitzpatrick R, Rogers DK, and McCloskey DI. Stable human standing with lower-limb muscle afferents providing the only sensory input. J Physiol 480 (Pt 2): 395-403, 1994.

Fitzpatrick RC, Taylor JL, and McCloskey DI. Ankle stiffness of standing humans in response to imperceptible perturbation: reflex and task-dependent components. J Physiol 454: 533-547, 1992a.

Fitzpatrick RC, Gorman RB, Burke D, and Gandevia SC. Postural proprioceptive reflexes in standing human subjects: bandwidth of response and transmission characteristics. J Physiol 458: 69-83, 1992b.

Fuglevand AJ, Winter DA, and Patla AE. Models of recruitment and rate coding organization in motor-unit pools. J Neurophysiol 70: 2470-2488, 1993.

Horak FB, and Macpherson JM. Postural orientation and equilibrium. In: Handbook of physiology. New York: Oxford University Press, 1996.

Ito T, Murano EZ, and Gomi H. Fast force-generation dynamics of human articulatory muscles. J Appl Physiol 96: 2318-2324; discussion 2317, 2004.

Jo S, and Massaquoi SG. A model of cerebellum stabilized and scheduled hybrid long-loop control of upright balance. Biol Cybern 91: 188-202, 2004.

Kawakami Y, Ichinose Y, and Fukunaga T. Architectural and functional features of human triceps surae muscles during contraction. J Appl Physiol 85: 398-404, 1998.

Lavoie BA, Cody FWJ, and Capaday C. Cortical control of human soleus muscle during volitional and postural activities studied using focal magnetic stimulation. Experimental Brain Research 103: 97-107, 1995.

Loram ID, and Lakie M. Direct measurement of human ankle stiffness during quiet standing: the intrinsic mechanical stiffness is insufficient for stability. J Physiol 545: 1041-1053, 2002.

Loram ID, Maganaris CN, and Lakie M. Active, non-spring-like muscle movements in

human postural sway: how might paradoxical changes in muscle length be produced? J Physiol 564: 281-293, 2005.

Loram ID, Maganaris CN, and Lakie M. Use of ultrasound to make noninvasive in vivo measurement of continuous changes in human muscle contractile length. J Appl Physiol 100: 1311-1323, 2006.

Mannard A, and Stein RB. Determination of the frequency response of isometric soleus muscle in the cat using random nerve stimulation. J Physiol 229: 275-296, 1973.

Masani K, Popovic MR, Nakazawa K, Kouzaki M, and Nozaki D. Importance of body sway velocity information in controlling ankle extensor activities during quiet stance. J Neurophysiol 90: 3774-3782, 2003.

Masani K, Vette AH, and Popovic MR. Controlling balance during quiet standing: proportional and derivative controller generates preceding motor command to body sway position observed in experiments. Gait Posture 23: 164-172, 2006a.

Masani K, Vette AH, Abe MO, Nakazawa K, and Popovic MR. Influence of the neuromuscular system on the control mechanism of balance during quiet standing. The 36th annual meeting of the Society for Neuroscience, Abstract 558.3, 2006b.

Mergner T, Maurer C, and Peterka RJ. A multisensory posture control model of human upright stance. Prog Brain Res 142: 189-201, 2003.

Morasso PG, Baratto L, Capra R, and Spada G. Internal models in the control of posture. Neural Networks 12: 1173-1180, 1999.

Morasso PG, and Sanguineti V. Ankle muscle stiffness alone cannot stabilize balance during quiet standing. J Neurophysiol 88: 2157-2162, 2002.

Morasso PG, and Schieppati M. Can muscle stiffness alone stabilize upright standing? J Neurophysiol 82: 1622-1626, 1999.

Panzer VP, Bandinelli S, and Hallett M. Biomechanical assessment of quiet standing and changes associated with aging. Arch Phys Med Rehabil 76: 151-157, 1995.

Peterka RJ. Postural control model interpretation of stabilogram diffusion analysis. Biol Cybern 82: 335-343, 2000.

Peterka RJ. Sensorimotor integration in human postural control. J Neurophysiol 88: 1097-1118, 2002.

Peterka RJ, and Loughlin PJ. Dynamic regulation of sensorimotor integration in human postural control. J Neurophysiol 91: 410-423, 2004.

Stein RB, French AS, Mannard A, and Yemm R. New methods for analysing motor function in man and animals. Brain Res 40: 187-192, 1972.

Tani H, and Nagasaki H. Contractile properties of human ankle muscles determined by a systems analysis method for the EMG-force relationship. J Electromyogr Kinesiol 6: 205-213, 1996.

van der Kooij H, Jacobs R, Koopman B, and Grootenboer H. A multisensory integration model of human stance control. Biol Cybern 80: 299-308, 1999.

van der Kooij H, Jacobs R, Koopman B, and van der Helm F. An adaptive model of sensory integration in a dynamic environment applied to human stance control. Biol Cybern 84: 103-115, 2001.

Vette AH, Masani K, and Popovic MR. Implementation of a physiologically identified PD feedback controller for regulating the active ankle torque during quiet stance. IEEE Trans Neural Sys Rehabil Eng 15:235-243, 2007.

Winter DA. Biomechanics and motor control of human movement. Hoboken: John Wiley & Sons, Inc., 2005.

Yamaguchi GT, Sawa AGU, Moran DW, Fessler MJ, and Winters JM. A survey of human musculotendon actuator parameters. In: Multiple muscle systems, edited by Winters JM, and Woo SL-Y. New York: Springer-Verlag, 1990, p. 716-773.

Zajac FE. Muscle and tendon: properties, models, scaling, and application to biomechanics and motor control. Crit Rev Biomed Eng 17: 359-411, 1989.

Table 1: Results of the optimization analysis. %Fit indicates the percentage of the goodness of fit between the measured and predicted ankle torque fluctuations. T indicates the twitch contraction time of the neuro-musculo-skeletal system, and ω_n indicates its natural frequency.

	%Fit		T	ω_n
Subject	Optimized Data	Validation Data	[s]	[rad/s]
A	86.2	77.1	0.121	8.30
B	93.7	93.6	0.133	7.51
C	82.6	83.7	0.187	5.33
D	89.6	88.0	0.124	8.08
E	94.1	94.2	0.192	5.21
F	86.2	81.3	0.147	6.82
G	92.0	91.8	0.148	6.77
H	94.9	90.6	0.163	6.12
Average	89.9	87.6	0.152	6.77
S.D.	4.5	6.2	0.027	1.17

Figure Legends

Fig. 1 Experimental setup of the support device. During SS and VS, the subject was supported by a support device from his/her front. The support device was ground-fixed and had a load cell built in. The subject stood on a force plate during all trials. A laser displacement sensor measured a point on the calf by which the ankle angle was calculated.

Fig. 2 Block diagram of the model used in the theoretical study. The model included a mechanical and a neural controller, an inverted pendulum representing human bipedal stance, transmission time delays, and the NMS torque generation process. The input to the NMS system was the delayed output of the neural controller corresponding to EMG, and the output of the NMS system corresponded to the active torque. The passive torque was provided by the mechanical controller and together with the active torque yielded the total ankle torque. m is the mass of the pendulum, h is the pendulum height, I is the moment of inertia of the pendulum, θ is the body angle, τ is the constant time delay, which was set to 80 ms. K_P and K_D are the gains for the neural controller, and K and B are the gains for the mechanical controller.

Fig. 3 Example recordings for one subject. From the top, the traces indicate the ankle angle, ankle torque, and EMGs of SOL, MG, LG, and TA. From the left, the records for FS, SS, VS and resting condition are shown. On the graphs of the ankle torque for SS and VS, the thin lines with $*$ indicate the torque provided by the load cell.

Fig. 4 A: Comparisons of the mean ankle torque in FS and VS and the mean torque provided by the support device in SS. B, C, D, and E: Comparison of the root mean squares of EMGs among FS, SS, VS and resting condition. SOL, MG, LG, TA indicate soleus

muscle, medial head of gastrocnemius, lateral head of gastrocnemius, and tibialis anterior muscle, respectively. The values indicate the group averages and the error bars indicate the standard deviations of the group. ∗ indicates $P<0.05$ among tasks.

Fig. 5 The power spectral density functions of SOL EMG (A) and the ankle torque (B) for all subjects in FS and VS.

Fig. 6 The measured ankle torque and the ankle torque estimated from SOL EMG (VS) using the identified neuro-musculo-skeletal system for one subject. (A) shows the plots for the optimized data, and (B) for the validation data. In the torque plots, the thin lines indicate the measured ankle torque, and the bold lines indicate the estimated ankle torque.

Fig. 7 The Bode plots and the time delay for each frequency component based on the phase plot of the identified NMS systems (A, B, C), and the empirical frequency response function for the same subject as in Fig. 6 (D, E). A: gain plots, B: phase plots, and C: time delay plots of the identified NMS system. The bold lines indicate the ones for $T = 0.152$ s, i.e., the group average value. The broken lines indicate the ones for $T = 0.121$ s, i.e., the group minimum value. The dotted lines indicate the ones for $T = 0.192$ s, i.e., the group maximum value. D: gain plot, and E: phase plot of the empirical frequency response function. The gain (G in eq. (1)) was set to 1 to isolate the frequency-specific properties of the transfer function.

Fig. 8 The gain combinations that stabilized the model with and without the identified NMS system. (A) shows the three-dimensional volume plot of the gain combinations of K_P, K_D and K that stabilized the entire model including the NMS system with $T = 0.152$ s. (B, C and D) represent the projections of the gain combinations onto the planes of K_P and K_D

(B), K_P and K (C), and K_D and K (D) that stabilized the entire model including the NMS system with $T = 0.121$ s (red +), $T = 0.152$ s (yellow ×), and $T = 0.192$ s (blue) . (E, F, and G) shows the projections of those gain combinations onto the planes of K_P and K_D (E), K_P and K (F), and K_D and K (G) that stabilized the entire model without the NMS system (grey area enclosed by dotted lines) compared to the stabilizing gain combinations with the NMS system (red +: $T = 0.121$ s, yellow ×: $T = 0.152$ s, and blue : $T = 0.192$ s). For all models, the viscosity B was set to 5 Nms/rad.

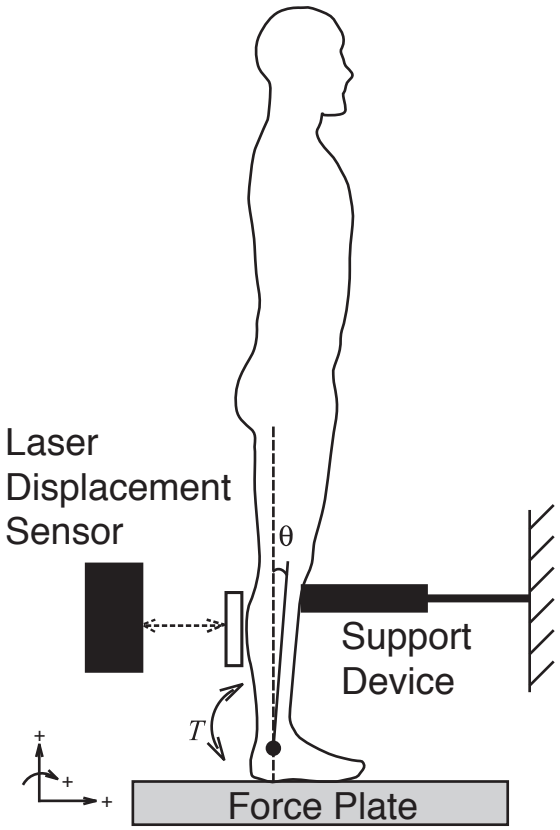
Laser
Displacement
Sensor
θ
Support
Device
T
+
+
+
Force Plate

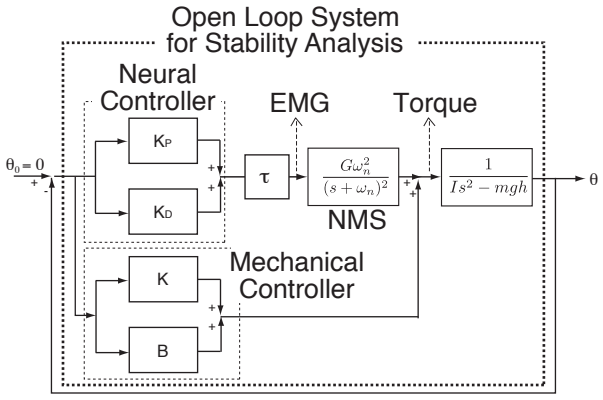
Open Loop System
for Stability Analysis
Neural
Controller
EMG
Torque
$\theta_0 = 0$
K_P
K_D
τ
$\frac{G\omega_n^2}{(s+\omega_n)^2}$
NMS
$\frac{1}{Is^2 - mgh}$
θ
Mechanical
Controller
K
B

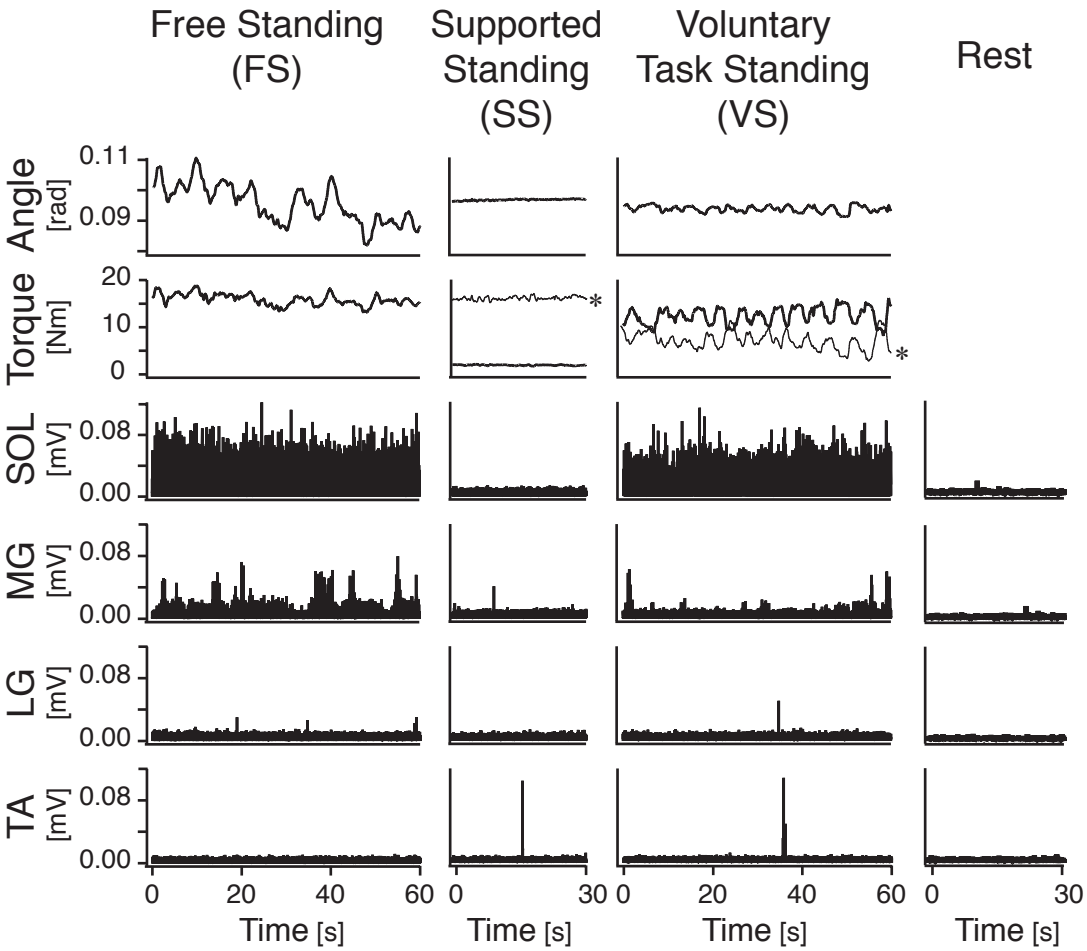
Free Standing (FS)
Supported Standing (SS)
Voluntary Task Standing (VS)
Rest
Angle [rad]
0.11
0.09
Torque [Nm]
20
10
0
*
*
SOL [mV]
MG [mV]
LG [mV]
TA [mV]
0.08
0.00
0
20
40
60
30
Time [s]

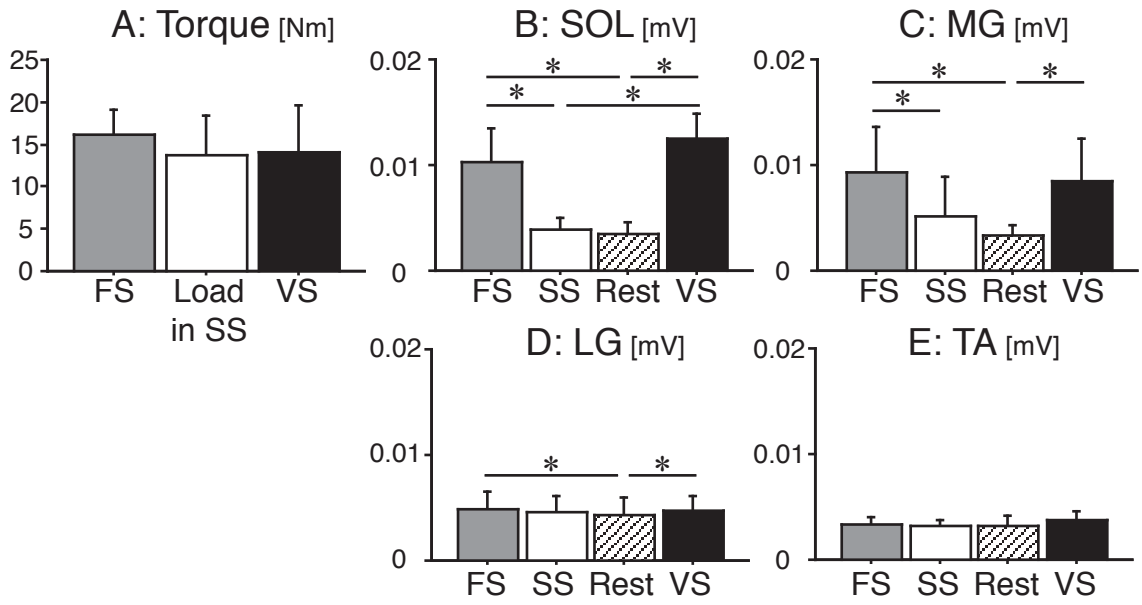
A: Torque [Nm]
25
20
15
10
5
0
FS
Load in SS
VS
B: SOL [mV]
0.02
0.01
0
FS
SS
Rest
VS
C: MG [mV]
0.02
0.01
0
FS
SS
Rest
VS
D: LG [mV]
0.02
0.01
0
FS
SS
Rest
VS
E: TA [mV]
0.02
0.01
0
FS
SS
Rest
VS

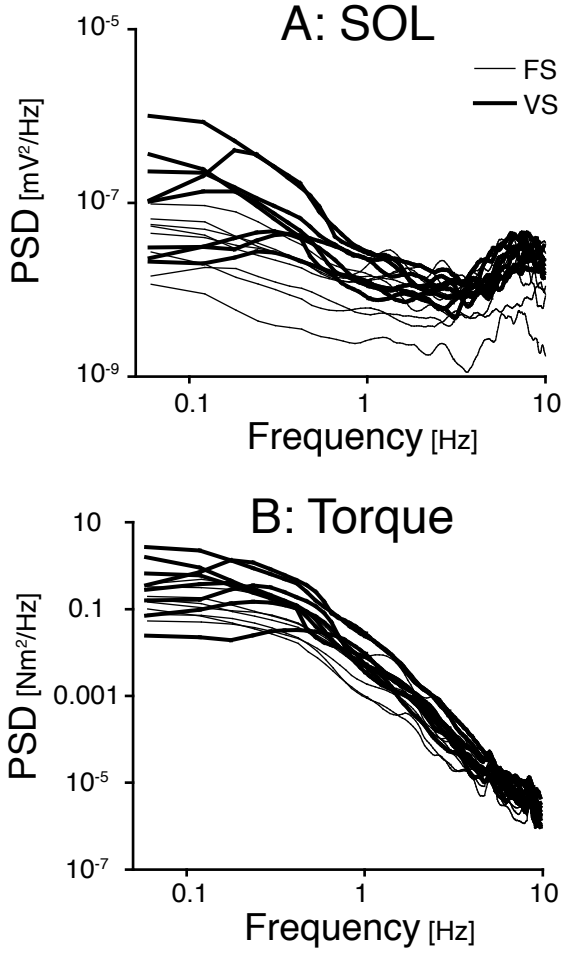
A: SOL
FS
VS
PSD [mV²/Hz]
10-5
10-7
10-9
0.1
1
10
Frequency [Hz]
B: Torque
PSD [Nm²/Hz]
10
0.1
0.001
10-5
10-7
0.1
1
10
Frequency [Hz]

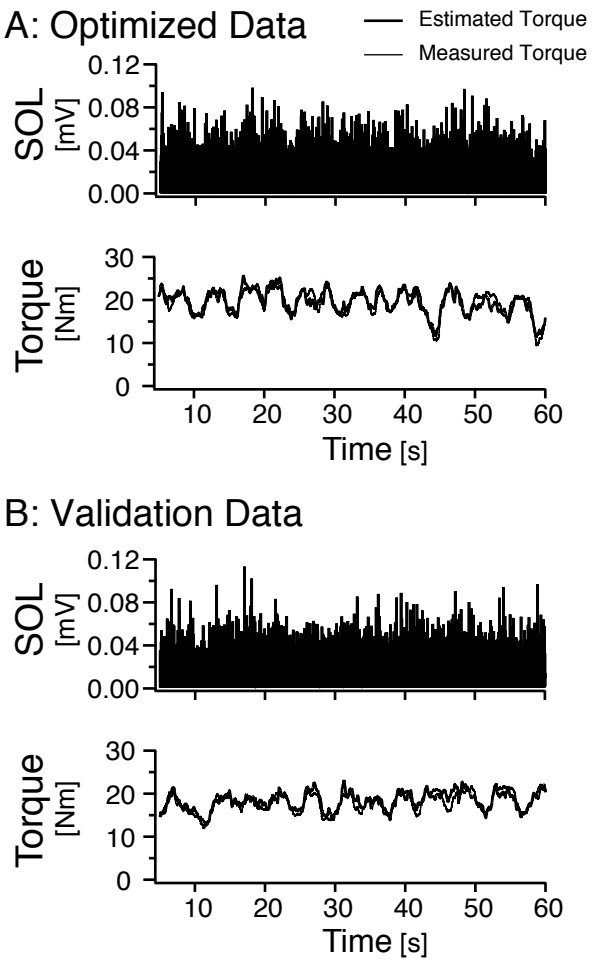
A: Optimized Data
Estimated Torque
Measured Torque
SOL [mV]
0.12
0.08
0.04
0.00
Torque [Nm]
30
20
10
0
10
20
30
40
50
60
Time [s]
B: Validation Data
SOL [mV]
0.12
0.08
0.04
0.00
Torque [Nm]
30
20
10
0
10
20
30
40
50
60
Time [s]

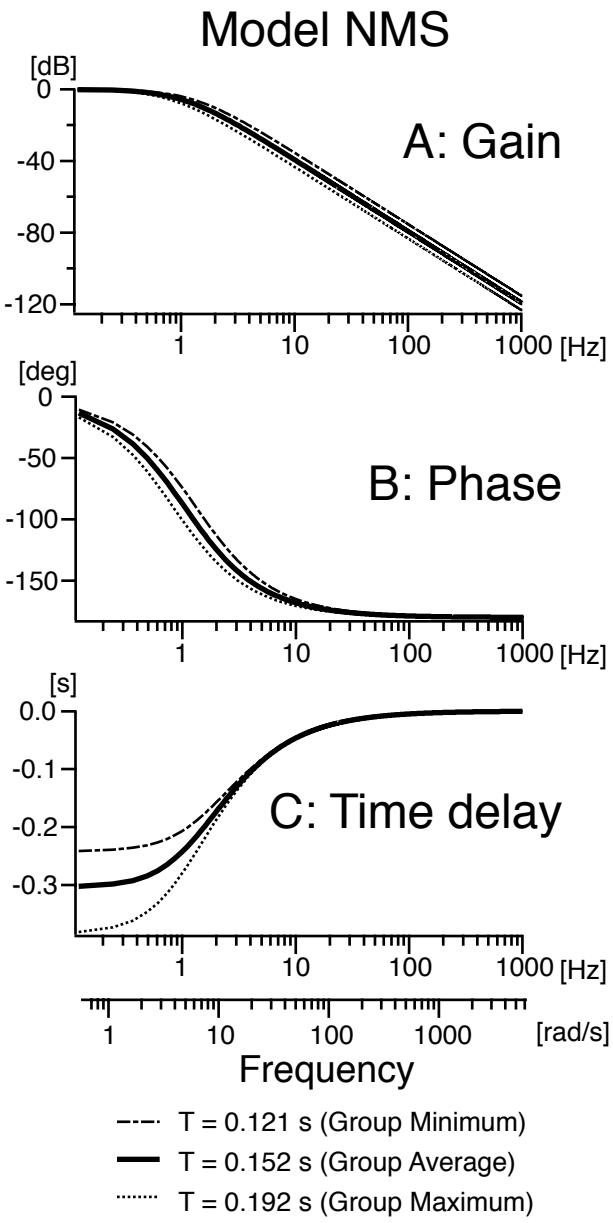
Model NMS
[dB]
0
-40
-80
-120
A: Gain
1
10
100
1000 [Hz]
[deg]
0
-50
-100
-150
B: Phase
1
10
100
1000 [Hz]
[s]
0.0
-0.1
-0.2
-0.3
C: Time delay
1
10
100
1000 [Hz]
1
10
100
1000
[rad/s]
Frequency
T = 0.121 s (Group Minimum)
T = 0.152 s (Group Average)
T = 0.192 s (Group Maximum)

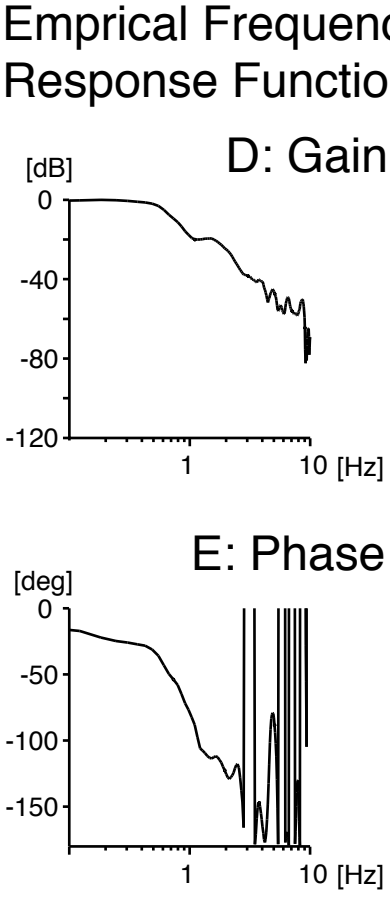
Emprical Frequency Response Function
D: Gain
[dB]
0
-40
-80
-120
1
10 [Hz]
E: Phase
[deg]
0
-50
-100
-150
1
10 [Hz]

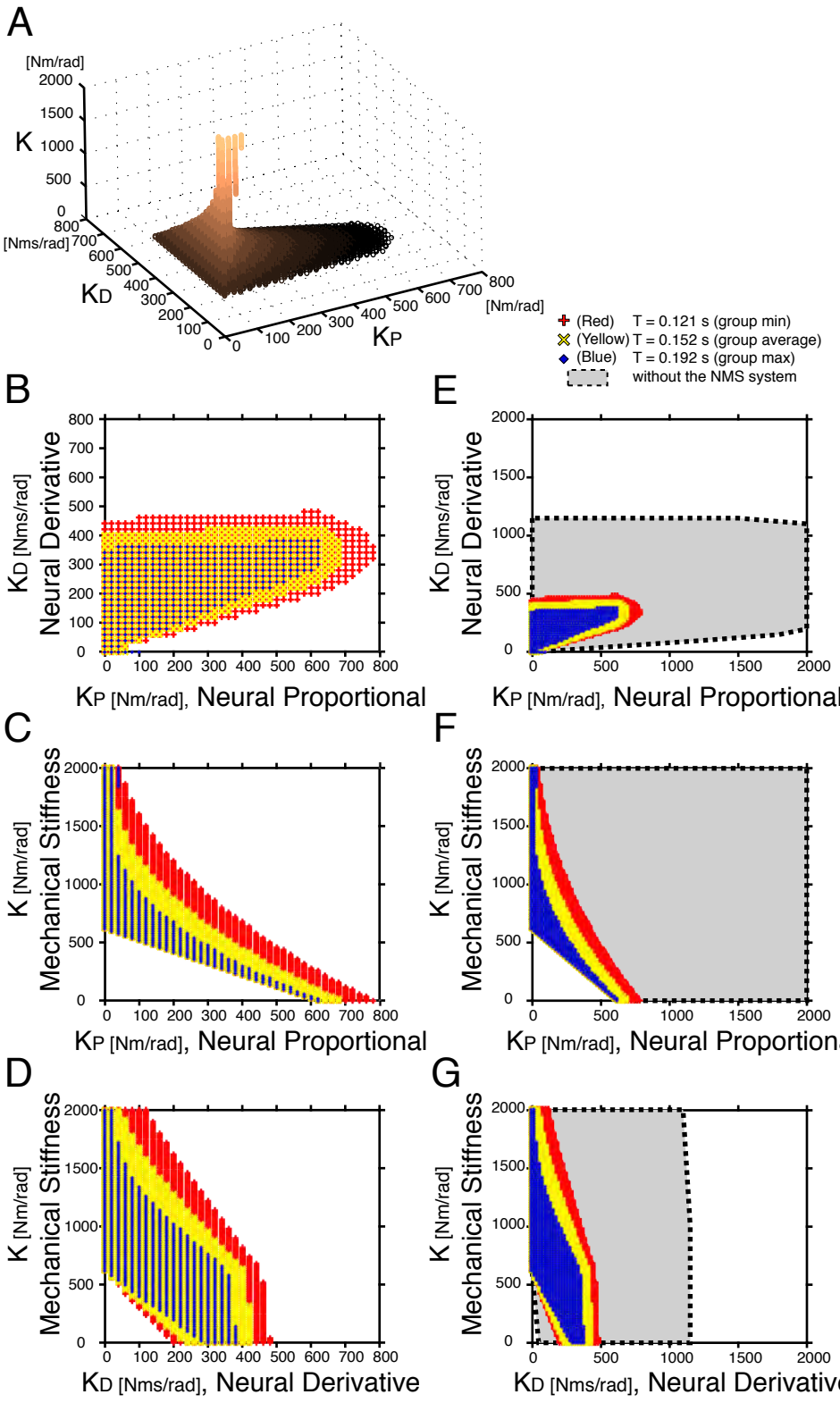
A
[Nm/rad]
K
[Nms/rad]
KD
KP
[Nm/rad]
(Red) T = 0.121 s (group min)
(Yellow) T = 0.152 s (group average)
(Blue) T = 0.192 s (group max)
without the NMS system
B
KD [Nms/rad] Neural Derivative
KP [Nm/rad], Neural Proportional
E
KD [Nms/rad] Neural Derivative
KP [Nm/rad], Neural Proportional
C
K [Nm/rad] Mechanical Stiffness
KP [Nm/rad], Neural Proportional
F
K [Nm/rad] Mechanical Stiffness
KP [Nm/rad], Neural Proportional
D
K [Nm/rad] Mechanical Stiffness
KD [Nms/rad], Neural Derivative
G
K [Nm/rad] Mechanical Stiffness
KD [Nms/rad], Neural Derivative